

# Effects of an Acid Catalyst on the Inorganic Domain of Inorganic–Organic Hybrid Materials

R. L. Ballard, S. J. Tuman, D. J. Fouquette, W. Stegmiller, and M. D. Soucek\*

Department of Polymers & Coatings, North Dakota State University,  
Fargo, North Dakota 58105

Received August 31, 1998. Revised Manuscript Received December 18, 1998

New inorganic–organic hybrid coatings have been developed using linseed oil and sunflower oil with the sol–gel precursor tetraethyl orthosilicate (TEOS). Hydrochloric acid (HCl) was used to catalyze the sol–gel reactions. The effects of HCl concentration on the morphology and distribution of the inorganic phase were investigated. Tensile properties, fracture toughness, thermogravimetric analysis (TGA), and dynamic mechanical thermal analysis (DMTA) of the ceramer coatings were evaluated as a function of acid catalyst concentration. In addition, scanning electron microscopy (SEM) and energy-dispersion X-ray analysis (EDAX) were used to investigate the morphology. The tensile properties showed an optimum acid concentration of 1.0 wt %. The fracture properties indicated that the greatest resistance to crack propagation was obtained with an acid concentration of 0.25 wt %. Thermogravimetric data showed that the thermal stability of the ceramer films increased with increasing acid catalyst. For TEOS/linseed ceramer films, storage modulus and  $\tan \delta$  data suggested that the acid catalyst promoted separation of the inorganic and organic phases. For TEOS/sunflower ceramer films, storage modulus and  $\tan \delta$  data suggested that the HCl promoted dispersion of the organic phase into the rigid inorganic phase.

## Introduction

The drastic differences in the chemistry and characteristics of ceramics and polymers have not allowed hybridization of the two materials until recently.<sup>1,2</sup> The major limitation of the traditional method of making an inorganic glass is that it involves a high-temperature (1200 °C) sintering process.<sup>2,3</sup> The sintering temperature is so high that it would degrade any organic polymer. A relatively new method for ceramic processing allows the hybridization of ceramics and polymers. This sol–gel process involves the formation of an inorganic glass from solution and allows low-temperature synthesis while yielding a high-purity homogeneous ceramic material.<sup>4,5</sup>

The sol–gel process can be used to make an inorganic–organic hybrid coating through the in situ polycondensation of a metal or silicon alkoxide in an organic polymer matrix.<sup>6,7</sup> The organic polymer matrix is formed by the oxidative cross-linking of a drying oil.<sup>7,8</sup> The inorganic microdomain is formed by hydrolysis, conden-

sation, and gelation of the metal or silicon alkoxide in solution. Some of the hydrolysis, condensation, and gelation mechanisms of this curing process are illustrated in Scheme 1 for a silicon alkoxide. Initial hydrolysis of the silicon alkoxide, **1**, results in partially hydrolyzed molecules, **2** and **3**. The partially hydrolyzed molecules can react with each other or with the silicon alkoxide through condensation to form larger molecules, **4** and **5**. Eventually, polycondensation results in a three-dimensional silica phase or gel, **6**.

Seed oils have traditionally been used as drying oils and as raw materials for uralkyds and alkyd resins.<sup>6,8</sup> Naturally occurring seed oils are triglycerides (triesters of glycerol) and fatty acids. The reactivity of these oils with oxygen results from the presence of esters of fatty acids with two or more double bonds that are either separated by single methylene groups or conjugated with each other. Esters of many different fatty acids occur in nature. Two important esters are those of linoleic acid and linolenic acid. Linoleic acid has one methylene group located between double bonds. Linolenic acid has two methylene groups located between double bonds.

Oils are typically classified as drying oils, semidrying oils, or nondrying oils, depending on the value of their drying index.<sup>7,8</sup> The drying index of an oil is equal to the weight percent of linoleic acid residues in the oil plus two times the weight percent of linolenic acid residues in the oil. If the drying index is greater than 70, the oil is classified a drying oil. If the drying index is in the range of 65–70, the oil is classified a semidrying oil. If the drying index is less than 65, the oil is classified a nondrying oil. Drying oils form solid films

\* To whom correspondence should be addressed.

(1) Brennan, A. B.; Wilkes, G. L. *Polymer* **1991**, *32*, 733.

(2) Noell, J. L. W.; Wilkes, G. L.; Mohanty, D. K.; McGrath, J. E. *J. Appl. Polym. Sci.* **1990**, *40*, 1177.

(3) Huang, H.-H.; Orler, B.; Wilkes, G. L. *Macromolecules* **1987**, *20*, 1322.

(4) Huang, H.-H.; Orler, B.; Wilkes, G. L. *Polym. Bull.* **1985**, *14*, 557.

(5) Brinker, C. J.; Scherer, G. W. *Sol–Gel Science, The Physics and Chemistry of Sol–Gel Processing*; Academic Press: New York, 1990.

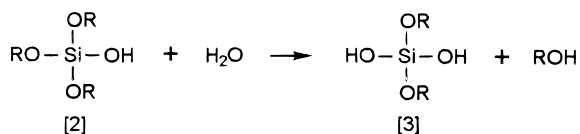
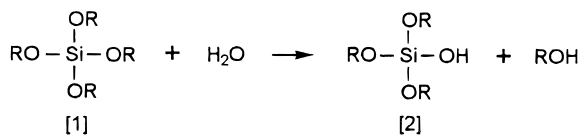
(6) Tuman, S. J.; Soucek, M. D. *J. Coat. Technol.* **1996**, *68*, 73.

(7) Wold, C. R.; Soucek, M. D. *J. Coat. Technol.* **1998**, *70*, 43.

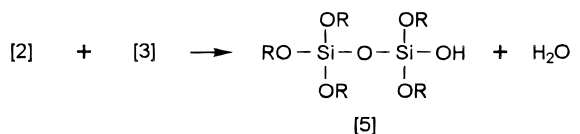
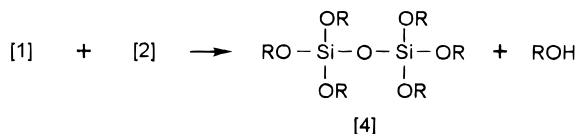
(8) Wicks, Jr., Z. W.; Jones, F. N.; Pappas, S. P. *Organic Coatings: Science and Technology, Volume I: Film Formation, Components, and Appearance*; John Wiley & Sons: New York, 1992.

### Scheme 1. Some of the Hydrolysis, Condensation, and Gelation Mechanisms of the Sol–Gel Curing Process for a Silicon Alkoxide

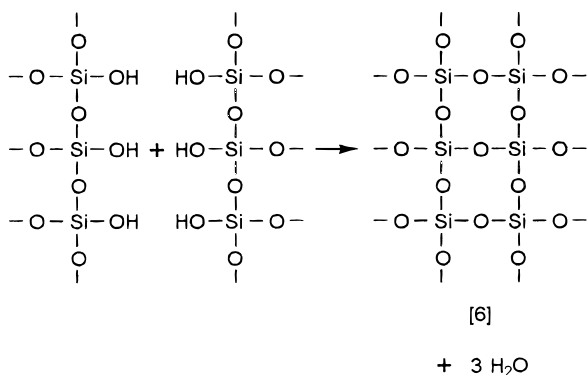
## Hydrolysis



## Condensation



## Gelation



on exposure to air. Semidrying oils form tacky, or sticky, films on exposure to air. Nondrying oils do not show a noticeable increase in viscosity on exposure to air.

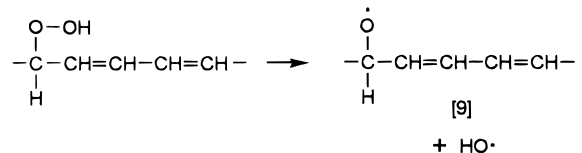
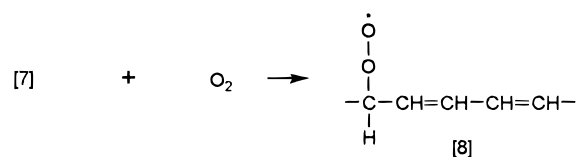
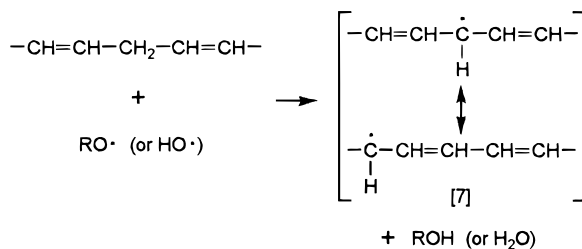
In drying oils, the unsaturated fatty acid residues cross-link through an oxidative reaction to form a coating.<sup>6,7</sup> Some of the initiation, propagation, and termination mechanisms of this process are illustrated in Scheme 2. In the initiation step, naturally occurring hydroperoxides decompose to form free radicals.<sup>8</sup> At first, these free radicals react mainly with naturally occurring antioxidants. As the antioxidants are consumed, the free radicals react with other compounds. Hydrogen atoms on methylene groups between double bonds are especially susceptible to abstraction, yielding resonance-stabilized free radical **7**. Free radical **7** reacts with oxygen to give predominantly a conjugated peroxy free radical such as **8**.<sup>8</sup> The peroxy free radicals can abstract hydrogen atoms from other methylene groups between double bonds to form additional hydroperoxides and regenerate free radicals such as **7**. These hydroperoxides can decompose to form free radicals with one oxygen atom such as **9**. Some of the cross-linking occurs

### Scheme 2. Some of the Initiation, Propagation, and Termination Mechanisms of the Curing Process for a Drying Oil

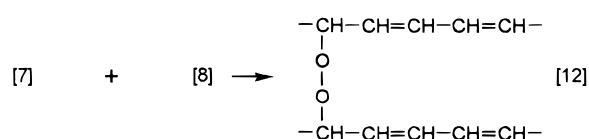
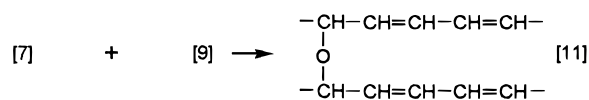
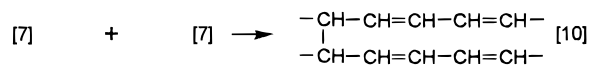
## Initiation



## Propagation



## Termination By Combination



by radical–radical combination reactions forming carbon–carbon (**10**), ether (**11**), and peroxide bonds (**12**).<sup>9</sup>

Metal catalysts, known as driers, can be added to accelerate the drying process.<sup>8,10</sup> The metal catalysts promote the decomposition of hydroperoxides.<sup>9,10</sup> This results in free radicals which initiate the oxidative polymerization process. Soucek and co-workers<sup>10</sup> investigated the effects of titanium alkoxide sol–gel precursors on the reaction kinetics of the auto-oxidative curing process and compared the effects to conventional driers. Differential scanning calorimetry (DSC) was used to study the effects of metal catalyst type and content on the auto-oxidative curing process of linseed oil. Zirconium and manganese were the conventional driers used. The inclusion of the zirconium and manganese driers lowered the temperature of the reaction exotherm for linseed oil. The titanium alkoxides produced results similar to those of the zirconium drier. While the

(9) Holmberg, K. *High Solids Alkyd Resins*; Marcel Dekker: New York, 1987.

(10) Tuman, S. J.; Chamberlain, D.; Scholsky, K. M.; Soucek, M. D. *Prog. Org. Coat.* **1996**, *28*, 251.

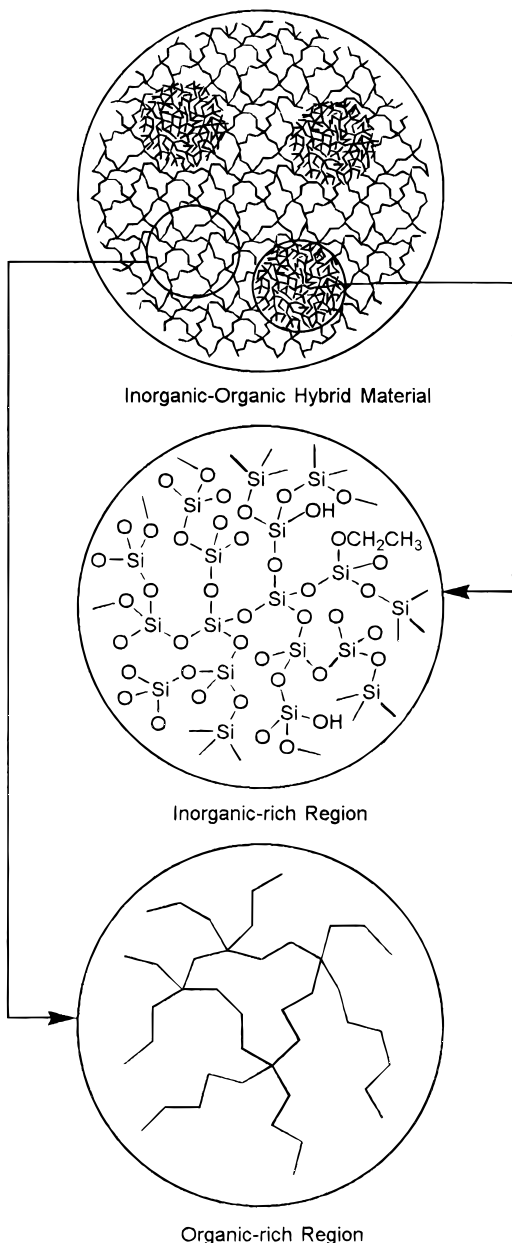
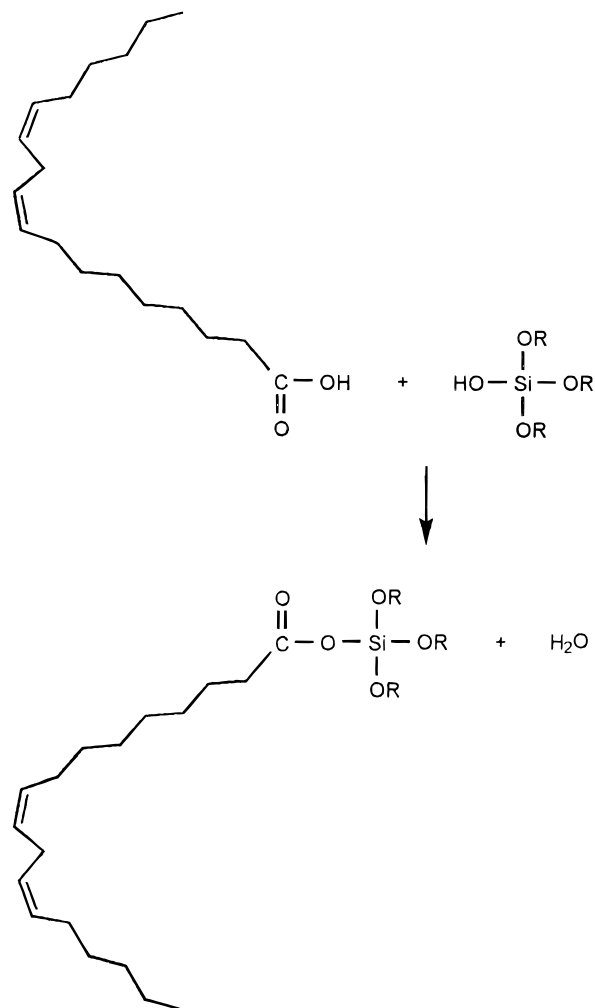


**Figure 1.** A theoretical structural model of an inorganic-organic hybrid material made with the sol-gel process.<sup>2</sup>

titanium alkoxides have the ability to catalyze the oxidative cross-linking of drying oils, tetraethyl orthosilicate (TEOS) does not act as a catalyst for this cross-linking.

One area of interest with these hybrid coatings is the control of the morphology of the inorganic clusters through the concentration of acid or base catalyst used.<sup>11,12</sup> Control of the size and distribution of the inorganic microdomain may lead to improved adhesion with metal substrates and improved corrosion protection.<sup>6,7</sup> The most effective method of controlling hydrolysis and condensation processes is to control the pH of the system.<sup>4,11</sup> An acidic or basic condition will have a great effect on the reaction paths of the sol-gel process and also on the structure of the condensed product. In

**Scheme 3.** Reaction of Free Fatty Acid with Hydrolyzed Silicon Alkoxide To Form an Inorganic-Organic Molecule



general, acid catalysis leads to a more polymeric form of gel with linear chains as intermediates, while base catalysis yields colloidal gels. A theoretical structural model of an inorganic-organic hybrid material made with the sol-gel process is shown in Figure 1.<sup>2</sup> The organic and inorganic molecules could form interpenetrating networks with no covalent bonding between organic and inorganic molecules. Another possibility is that covalent bonding could occur by saponification of the fatty acid esters of the drying oil and subsequent reaction with hydroxides on the inorganic molecules. Free fatty acids could also form a link between the organic and inorganic phases.<sup>13</sup> Free fatty acids could react with hydrolyzed silicon alkoxide molecules to form inorganic-organic molecules as shown in Scheme 3. The inorganic end of the molecule could become part of the silicon oxide gel. The organic end of the molecule could become part of the organic polymer matrix through its double bonds.

Wilkes and co-workers<sup>3,4</sup> studied the effect of acid content on hybrid materials made from tetraethyl orthosilicate (TEOS) and poly(dimethylsiloxane) (PDMS). Dynamic mechanical tests indicated that a portion of the siloxane species was phase separated, while the

(11) Wang, S.; Mark, J. E. *Macromol. Rep.* **1994**, A31(SUPPL. 3-4), 253.

(12) Kaddami, H.; Surivet, F.; Gerard, J. F.; Lam, T. M.; Pascault, J. P. *J. Inorg. Organomet. Polym.* **1994**, 4, 183.

(13) Sailer, R. A.; Soucek, M. D. *Prog. Org. Coat.* **1998**, 33, 36.

remainder was well dispersed. The effect of acid content was significant on the dispersion of the siloxane components and on the structure and properties of the final products. Small-angle X-ray scattering (SAXS) measurements indicated that an increase in acid content shortens the period for self-condensation of PDMS and results in a material with more dispersed oligomers. As a result, the final product becomes more homogeneous and shows higher extensibility.

Brennan and Wilkes<sup>1</sup> used poly(styrene sulfonic acid) to prepare hybrid materials based upon poly(tetramethylene oxide) oligomers and TEOS. The mechanical properties of the polymeric-acid-catalyzed materials were improved over systems of the same composition catalyzed with hydrochloric acid (HCl). The general morphological features of these materials, evaluated by dynamic mechanical and SAXS measurements, were quite similar to those of hybrid materials catalyzed with HCl. The use of the polymeric acid catalyst promoted a higher level of condensation in the hybrid materials. Observed changes in the sol viscosity upon addition of these catalysts indicated a possible method for modification of the rheological behavior of the sols.

Mark and co-workers<sup>14</sup> prepared very tough reinforced elastomers by swelling cured PDMS networks with TEOS and hydrolyzing the TEOS in situ to form silica particles. It was also possible to simultaneously cure and fill a PDMS network by reacting PDMS, TEOS, and water.<sup>15</sup> In another study, Mark and Wang<sup>11</sup> were able to control the distribution of silica particles produced by a sol-gel precipitation process through their choice of catalyst. A base catalyst produced well-distributed particles and an acid catalyst caused the silica to precipitate near the surface with essentially none in the interior. The results underscored the importance of controlling mass-transport phenomena and reaction conditions during the in situ generation of silica.

Lam and co-workers<sup>12</sup> prepared hybrid organic-inorganic materials based on a hydrogenated polybutadiene macromonomer. The final morphology of the cured hybrid materials depended on the amount of acid catalyst used and indicated that the acid concentration modified not only the rate of hydrolysis of the alkoxide but also the structure of the final hybrid material. For high acid concentrations, only one relaxation peak was observed by dynamic mechanical spectroscopy. For a low acid concentration, two relaxation peaks were observed by dynamic mechanical spectroscopy, indicating microphase separation. One relaxation was attributed to the organic-rich phase and the other relaxation was attributed to the mixed interfacial region between the organic phase and the inorganic-rich clusters. The final morphology was the result of competition between the kinetics of polymerization and the kinetics of microphase separation. When the polymerization went slowly at the low acid concentration, the entire microphase separation had enough time to take place.

In this study, TEOS was incorporated into linseed oil and sunflower oil coatings. Tensile properties, fracture

toughness, thermal stability, and dynamic mechanical properties were measured for these ceramer coatings. Scanning electron microscopy and energy-dispersion X-ray analysis were used to study the morphology of a linseed oil based ceramer coating. The effects of acid catalyst concentration on the morphology and distribution of the inorganic microdomain were observed.

## Experimental Section

The linseed oil used in this study was obtained from Frost Paint and Oil Corp. (Chicago, IL). The sunflower oil was obtained from National Sun Industries (Fargo, ND). Huls America (Piscataway, NJ) provided the zirconium drier. The TEOS ( $\text{Si}(\text{OCH}_2\text{CH}_3)_4$ ) was obtained from Strem Chemicals (Newburyport, MA). The HCl was obtained from Curtin Matheson Scientific, Inc. (Eden Prairie, MN). All materials were used as received.

Each sample was named according to its components. For example, consider the sample designated LIN-TEOS(25)-Zr(1.0)-HCl(2.0). The first two terms, LIN-TEOS(25), indicate that the material was made from a mixture of 75 wt % linseed oil and 25 wt % TEOS. The third term, Zr(1.0), indicates that the weight of zirconium drier added was 1.0% of the weight of the drying oil. The fourth term, HCl(2.0), indicates that the weight of HCl catalyst added was 2.0% of the weight of the sol-gel precursor.

A resin solution of each sample was prepared by mixing the appropriate quantities of drying oil, sol-gel precursor, drier, and catalyst. The acid catalyst was added dropwise to the sol-gel precursor. A separate solution was made by adding the drier dropwise to the drying oil. The two solutions were then mixed together and stirred 10–15 min. Films were cast on Pyrex glass plates using a casting blade set at 80–140  $\mu\text{m}$  thickness. The glass plates were then placed in a dust-free drying chamber at room temperature for 48 h. This allowed the 2-propanol present in the sol-gel precursor solution to evaporate before the films were cured in an oven. The cure cycle for the films was 1 h at 130 °C, 1 h at 180 °C, and 1 h at 210 °C. The films were slowly cooled to room temperature and then soaked in deionized water for 48 h. Once removed from the glass plates, the dry films were 30–90  $\mu\text{m}$  thick.

Tensile measurements were made on dogbone-shaped specimens with a thickness of 70–90  $\mu\text{m}$  and a width of 12 mm at the center. The initial gauge length was 4–5 cm. The testing was performed on an Instron Universal Tester Model 1000. A crosshead speed of 2 mm/min was used to measure tensile strength, strain-at-break, and tensile modulus. More than five samples were tested for each composition and average values are reported.

Plane-stress fracture toughness tests were conducted on rectangular specimens with a single-edge-notch (SEN) geometry. Rectangular strips 13 mm wide were cut from each material with sharp scissors. Each strip was supported on lightweight cardboard and cut with a razor blade to create the edge notch. This procedure gave a crack which appeared sharp under a microscope. A fracture toughness tester which was mounted on a microscope stage and equipped with a 25 lb (111 N) load cell and a variable speed motor was used to deform the specimen in a tensile mode. The load-displacement curve for each test was recorded on a chart recorder. The crack tip region was observed at a magnification of 220 $\times$ , and the onset of crack propagation was noted and marked on the load-displacement curve. The deformation zone near the crack tip could be observed continuously during the loading.

The plane-stress fracture toughness (stress intensity factor at fracture) was calculated using the following equation:<sup>16</sup>

(14) Ning, Y.-P.; Tang, M.-Y.; Jiang, C.-Y.; Mark, J. E.; Roth, W. *J. Appl. Polym. Sci.* **1984**, *29*, 3209.

(15) Mark, J. E.; Jiang, C.-Y.; Tang, M.-Y. *Macromolecules* **1984**, *17*, 2613.

(16) Williams, J. G. *Fracture Mechanics of Polymers*; John Wiley & Sons: New York, 1987.



$$K_c = [3.94(2w/\pi a) \tan(\pi a/2w)]^{1/2} a^{1/2} [F/(w-a)b] \quad (1)$$

where  $K_c$  is the plane-stress fracture toughness,  $w$  is the sample width,  $a$  is the notch length,  $F$  is the force on the sample when crack propagation begins, and  $b$  is the sample thickness. The energy release rate per unit crack area at fracture was calculated using the following equation:<sup>16</sup>

$$G_c = K_c^2/E \quad (2)$$

where  $G_c$  is the energy release rate per unit crack area at fracture,  $K_c$  is the plane-stress fracture toughness, and  $E$  is the tensile modulus (Young's modulus). Each of the fracture toughness data points reported represents the average of at least five samples. The energy release rate values were calculated using average values of fracture toughness and tensile modulus.

Dynamic thermogravimetric analysis (TGA) was performed on a DuPont 951 thermogravimetric analyzer with Thermal Analyst 2000 software. Typical sample weights for TGA measurements were 8–10 mg. The samples were heated from 100 to 550 °C at a rate of 20 °C/min with an air purge rate of 10 mL/min. Scanning electron microscopy (SEM) was performed with a JEOL JSM 6300V scanning electron microscope, with inclusion of energy-dispersion X-ray analysis (EDAX). Dynamic mechanical thermal analysis (DMTA) was performed with a Rheometric Scientific DMTA 3E. The samples were tested at a frequency of 1 Hz in the temperature range from –100 to 200 °C with a heating rate of 3 °C/min.

The cross-link density of the films was calculated using the following equation:<sup>17</sup>

$$\nu_e = E'_{\min}/(3RT) \quad (3)$$

where  $\nu_e$  is the cross-link density of elastically effective network chains,  $E'_{\min}$  is the minimum value of the storage modulus well above the glass transition temperature ( $T_g$ ),  $R$  is the gas constant, and  $T$  is the absolute temperature. This equation is valid for temperatures well above  $T_g$  where the loss modulus ( $E''$ ) is low and the modulus ( $E'$ ) is approximately equal to the storage modulus ( $E'$ ). An elastically effective network chain is connected at both ends to the network at different junction points. Short cyclical chains and dangling ends are not elastically effective. In the systems of this study, the cross-links are predominantly drying-oil cross-links, but there could be some inorganic-phase cross-links if the inorganic phase is connected to the organic phase.

## Results and Discussion

The primary objective of this study was to investigate the effects of an acid catalyst on phase morphology and microdomain distribution in sol–gel–drying-oil hybrid coatings. Our long-term goal is to develop low-VOC (volatile organic compounds), chromate-free, corrosion-resistant primers for metal substrates that will provide better adhesion than current primers with minimal environmental impact. The sol–gel inorganic component of these coatings can react with the metal substrate, protecting it from oxidation. The major driving force of this project is to replace chromate-based coatings. Restrictions on chromates have led to research on chromate-free anticorrosion barrier coatings.

An attempt was made to incorporate TEOS into linseed oil and sunflower oil coatings without a catalyst, but the TEOS vaporized from the coatings at elevated temperatures before polycondensation could occur. El-

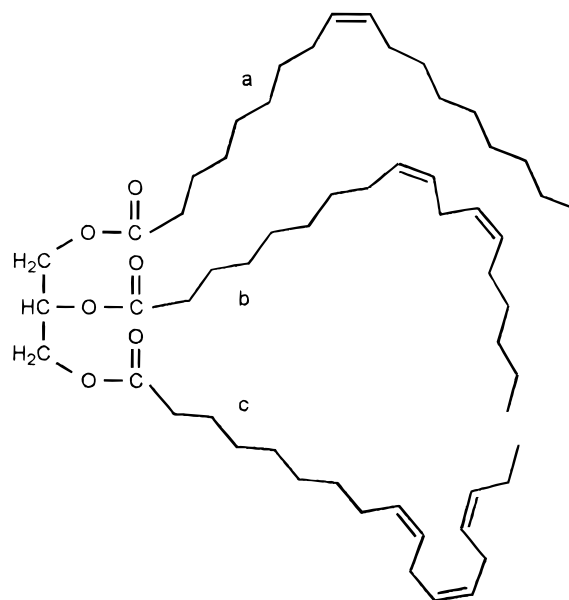


**Figure 2.** An example of one of the many triglycerides in linseed oil. This triglyceride contains (a) oleic, (b) linoleic, and (c) linolenic acid residues.

**Table 1.** the Fatty Acid Compositions of the Linseed Oil and Sunflower Oil Used in This Study

oil	fatty acid residues (wt %)			
	saturated	oleic	linoleic	linolenic
linseed	10	22	16	52
sunflower	13	17	70	0

emental analysis confirmed the absence of silicon in TEOS/drying oil hybrid coatings without a catalyst. The initial part of this study utilized an acid catalyst to initiate hydrolysis and condensation of the TEOS at ambient temperature. The tensile properties, fracture toughness, thermal stability, and dynamic mechanical properties of the TEOS/drying oil coatings were observed as a function of acid concentration. The weight ratio of sol–gel precursor to drying oil was held constant at 25 to 75, while the weight percent of acid in the sol–gel precursor was varied from 0.0 to 3.0. The second part of this study utilizes SEM with EDAX to observe the morphology and distribution of the inorganic domain in the LIN-TEOS(25)-Zr(1.0)-HCl(3.0) system. The zirconium drier was included since TEOS does not catalyze the oxidative polymerization of the drying oil.

The linseed oil used in this study had a drying index of 120. The sunflower oil had a drying index of 70. The linseed oil was chosen for its high concentration of linolenic acid (52 wt %). The sunflower oil was chosen for its high linoleic acid content (70 wt %) and its lack of linolenic acid. Methylene groups between double bonds are reactive sites for cross-linking. Linolenic acid has two doubly allylic methylene groups, while linoleic acid has only one. As a result, linseed oil will undergo faster cross-linking than sunflower oil under the same conditions. Inorganic–organic hybrid coatings based on linseed oil would be expected to have higher cross-link densities than analogous inorganic–organic hybrid coatings based on sunflower oil. The fatty acid compositions of the linseed oil and sunflower oil used in this study are shown in Table 1. An example of one of the many triglycerides in linseed oil is shown in Figure 2.

(17) Wicks, Jr., Z. W.; Jones, F. N.; Pappas, S. P. *Organic Coatings: Science and Technology, Volume II: Applications, Properties, and Performance*; John Wiley & Sons: New York, 1994.

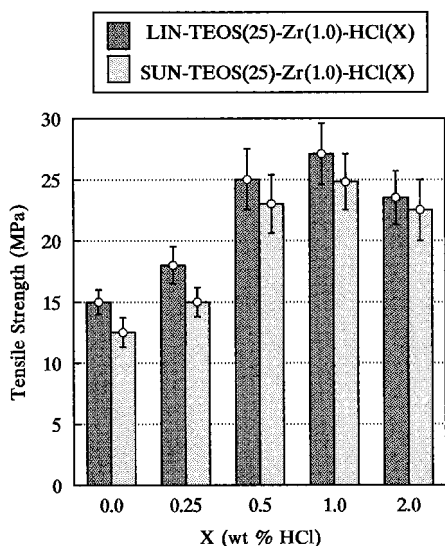


**Figure 3.** Tensile strength as a function of HCl concentration for TEOS/linseed oil and TEOS/sunflower oil films.

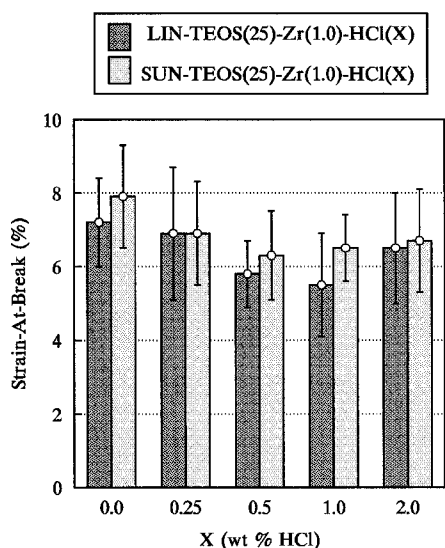


**Figure 4.** Strain-at-break as a function of HCl concentration for TEOS/linseed oil and TEOS/sunflower oil films.

The tensile strength of TEOS/linseed oil and TEOS/sunflower oil films is shown in Figure 3 as a function of HCl concentration. The tensile strength of both types of films increased with the acid concentration up to 1.0 wt % HCl and decreased at 2.0 wt % HCl. The maximum tensile strength at 1.0 wt % HCl was 27.1 MPa for TEOS/linseed oil films and 24.8 MPa for TEOS/sunflower oil films. These tensile strengths are higher than those of linseed oil and sunflower oil films containing only 1.0 wt % zirconium drier.<sup>6</sup>

Figure 4 shows the strain-at-break for TEOS/linseed oil and TEOS/sunflower oil films as a function of HCl concentration. The strain-at-break values for both types of films were fairly constant over the entire acid concentration range. There was only a slight difference between the strain-at-break values for the TEOS/linseed oil films and the analogous TEOS/sunflower oil films. The minimum strain-at-break for the TEOS/linseed oil films was 5.5% at 1.0 wt % HCl. The minimum strain-at-break for the TEOS/sunflower oil films was 6.3% at 0.5 wt % HCl. The strain-at-break values for linseed oil and sunflower oil films containing 1.0 wt % zirconium

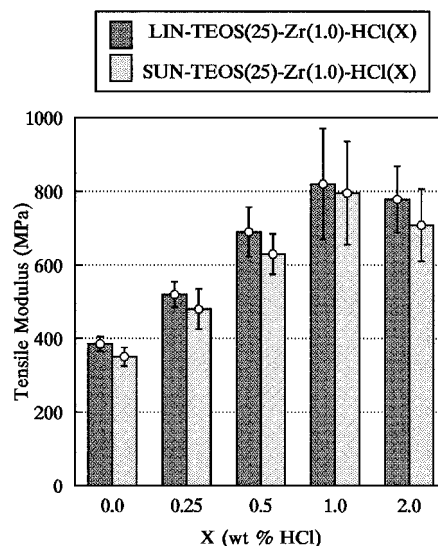


**Figure 5.** Tensile modulus as a function of HCl concentration for TEOS/linseed oil and TEOS/sunflower oil films.

drier are approximately the same as the strain-at-break values obtained in this study.<sup>6</sup>

The tensile modulus of TEOS/linseed oil and TEOS/sunflower oil films is shown in Figure 5 as a function of HCl concentration. The tensile modulus of both types of films increased with the acid concentration up to 1.0 wt % HCl and decreased at 2.0 wt % HCl. The maximum tensile modulus at 1.0 wt % HCl was 820 MPa for TEOS/linseed oil films and 795 MPa for TEOS/sunflower oil films. These modulus values are higher than those of linseed oil and sunflower oil films containing only 1.0 wt % zirconium drier.<sup>6</sup>

Since the composition of the films was held constant except for the acid catalyst, the changes in tensile strength and tensile modulus were caused by changes in the size and distribution of the inorganic clusters. There appears to be an optimum concentration of acid catalyst at 1.0 wt %. This concentration yielded the strongest films with a high tensile modulus. When the properties of the TEOS/drying oil films are compared to earlier results,<sup>6</sup> it can be seen that the TEOS films are stronger than films containing only zirconium drier. This is due to the presence of the inorganic phase produced by the TEOS. The tensile properties of TEOS/drying oil films are similar to the tensile properties of drying oil based films containing titanium diisopropoxide bis(acetylacetonate) (TIA) and titanium(IV) isopropoxide (TIP).<sup>6</sup>

The plane-stress fracture toughness ( $K_c$ ) of TEOS/linseed oil and TEOS/sunflower oil films is shown in Figure 6 as a function of HCl concentration. The maximum fracture toughness for both the TEOS/linseed oil and TEOS/sunflower oil films occurred at 0.25 wt % HCl. The fracture toughness values for both types of films were fairly constant over the rest of the acid concentration range. The maximum fracture toughness for the TEOS/linseed oil films was 1.63 MPa(m)<sup>1/2</sup>. The maximum fracture toughness for the TEOS/sunflower oil films was 0.79 MPa(m)<sup>1/2</sup>. These maximum values for fracture toughness are 3–7 times higher than the fracture toughness values of analogous films with 25 wt % TIA or TIP.<sup>18</sup> They are 2 times higher than the fracture toughness values of analogous films containing only 1.0 wt % zirconium drier.<sup>18</sup>

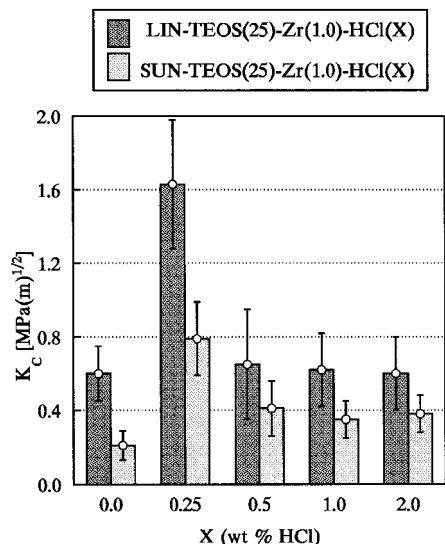


**Figure 6.** Plane-stress fracture toughness ( $K_c$ ) as a function of HCl concentration for TEOS/linseed oil and TEOS/sunflower oil films.

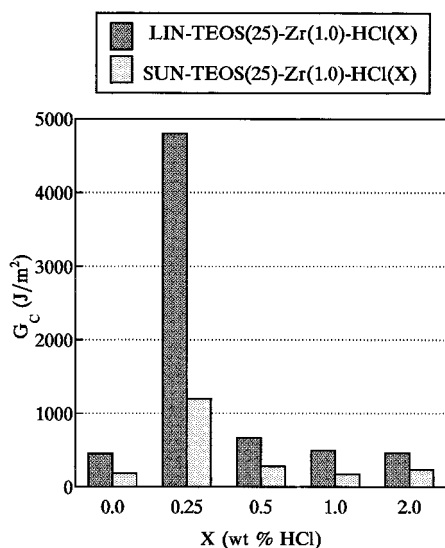


**Figure 7.** Energy release rate per unit crack area at fracture ( $G_c$ ) as a function of HCl concentration for TEOS/linseed oil and TEOS/sunflower oil films.

Figure 7 shows the energy release rate per unit crack area at fracture ( $G_c$ ) for TEOS/linseed oil and TEOS/sunflower oil films as a function of HCl concentration. The maximum energy release rate for both the TEOS/linseed oil and TEOS/sunflower oil films occurred at 0.25 wt % HCl. The energy release rate values for both types of films were fairly constant over the rest of the acid concentration range. The maximum energy release rate for the TEOS/linseed oil films was 4800 J/m<sup>2</sup>. The maximum energy release rate for the TEOS/sunflower oil films was 1200 J/m<sup>2</sup>. These maximum energy release rates are 9–80 times higher than the energy release rates for analogous films with 25 wt % TIA or TIP.<sup>18</sup> They are 3 times higher than the energy release rates for analogous films containing only 1.0 wt % zirconium drier.<sup>18</sup>

The fracture toughness and energy release rate are a measure of resistance to crack extension. Although

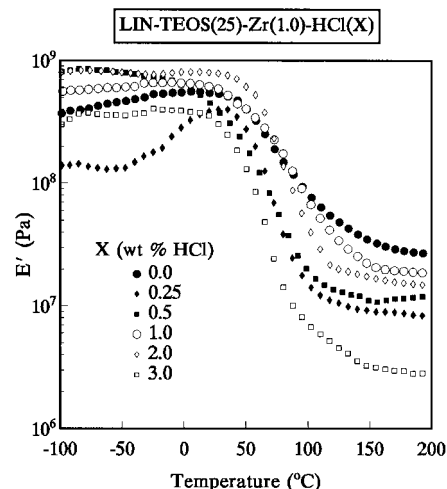


**Figure 8.** Storage modulus ( $E'$ ) as a function of temperature for TEOS/linseed oil films differing in HCl concentration.

**Table 2. Thermogravimetric Analysis (TGA) Data for TEOS/Linseed Oil and TEOS/Sunflower Oil Films Differing in HCl Concentration**

sample	temperature (°C) required to produce % weight loss			
	5%	10%	25%	50%
LIN-TEOS(25)-Zr(1.0)-HCl(0.0)	279	295	340	378
LIN-TEOS(25)-Zr(1.0)-HCl(0.25)	281	283	321	407
LIN-TEOS(25)-Zr(1.0)-HCl(0.5)	294	316	358	432
LIN-TEOS(25)-Zr(1.0)-HCl(1.0)	287	308	357	443
LIN-TEOS(25)-Zr(1.0)-HCl(2.0)	299	317	366	450
SUN-TEOS(25)-Zr(1.0)-HCl(0.0)	277	283	303	358
SUN-TEOS(25)-Zr(1.0)-HCl(0.25)	271	293	331	417
SUN-TEOS(25)-Zr(1.0)-HCl(0.5)	289	309	345	427
SUN-TEOS(25)-Zr(1.0)-HCl(1.0)	287	299	337	427
SUN-TEOS(25)-Zr(1.0)-HCl(2.0)	285	311	356	444

the tensile properties indicate an optimum acid concentration of 1.0 wt %, the fracture properties indicate that the greatest resistance to crack propagation is obtained with an acid concentration of 0.25 wt %. These differing results demonstrate the usefulness of fracture toughness testing. Even though a material can withstand a given tensile load while intact, it may not resist failure by crack propagation.

TGA data for the TEOS/linseed oil and TEOS/sunflower oil films are shown in Table 2. The initial 5% weight loss for all the samples occurred between 270 and 300 °C. Both types of films showed a significant increase in the temperature required to produce a 50% weight loss as the acid concentration was increased. Weight loss from the films may be attributed to the decomposition of the drying oil cross-links or to the vaporization or decomposition of byproducts from the hydrolysis and condensation of the sol-gel precursor.

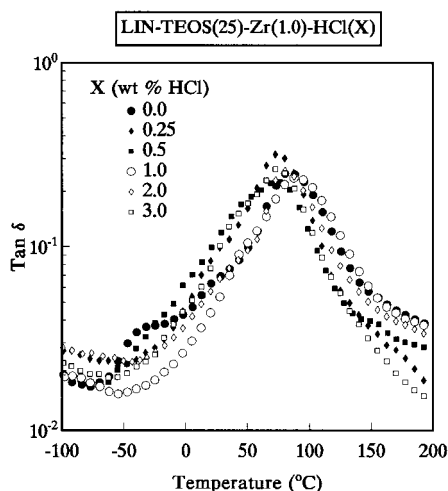
Storage modulus ( $E'$ ) is shown in Figure 8 as a function of temperature for TEOS/linseed oil films differing in HCl concentration. The samples containing acid had lower values of high-temperature storage modulus than the sample containing no acid. The sample with 3.0 wt % HCl had the lowest value for the high-temperature storage modulus. The minimum values of storage modulus and the corresponding cross-link densities calculated using eq 3 are shown in Table 3. The presence of the acid decreased the cross-link density. For the acid containing samples, the sample with 1.0 wt % HCl had the highest cross-link density.

(18) Tuman, S. J., M.S. Thesis, North Dakota State University, 1995.



**Table 3. Dynamic Mechanical Thermal Analysis (DMTA) Data for TEOS/linseed Oil and TEOS/Sunflower Oil Films Differing in HCl Concentration**

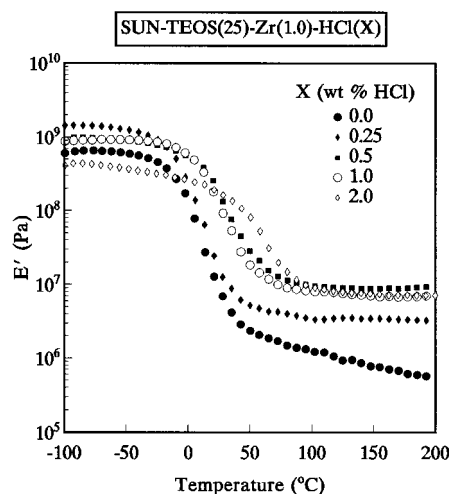
sample	$E_{\min}$ (Pa)	temp ( $^{\circ}$ C) for $E_{\min}$	$\nu_e$ (mol/m <sup>3</sup> )	$T_g$ ( $^{\circ}$ C) from tan $\delta$ peak
LIN-TEOS(25)-Zr(1.0)-HCl(0.0)	$2.70 \times 10^7$	191.1	2330	83.6
LIN-TEOS(25)-Zr(1.0)-HCl(0.25)	$7.98 \times 10^6$	200.1	676	74.3
LIN-TEOS(25)-Zr(1.0)-HCl(0.5)	$1.07 \times 10^7$	156.7	998	73.2
LIN-TEOS(25)-Zr(1.0)-HCl(1.0)	$1.80 \times 10^7$	199.6	1530	89.4
LIN-TEOS(25)-Zr(1.0)-HCl(2.0)	$1.47 \times 10^7$	200.1	1250	80.3
LIN-TEOS(25)-Zr(1.0)-HCl(3.0)	$2.78 \times 10^6$	195.6	238	74.1
SUN-TEOS(25)-Zr(1.0)-HCl(0.0)	$5.07 \times 10^5$	194.1	44	14.7
SUN-TEOS(25)-Zr(1.0)-HCl(0.25)	$3.23 \times 10^6$	196.6	276	15.8
SUN-TEOS(25)-Zr(1.0)-HCl(0.5)	$8.72 \times 10^6$	143.1	840	36.6
SUN-TEOS(25)-Zr(1.0)-HCl(1.0)	$6.74 \times 10^6$	169.6	610	32.8
SUN-TEOS(25)-Zr(1.0)-HCl(2.0)	$7.05 \times 10^6$	166.8	642	58.2

**Figure 9.** tan  $\delta$  as a function of temperature for TEOS/linseed oil films differing in HCl concentration.

The transition regions of the samples containing acid were steeper than the transition region of the sample containing no acid, indicating that the acid narrowed the transition region. The transition regions were also shifted to lower temperatures.

Figure 9 shows tan  $\delta$  as a function of temperature for TEOS/linseed oil films differing in HCl concentration. The samples containing acid had narrower transition peaks than the sample containing no acid. The glass transition temperatures determined from the tan  $\delta$  peaks are shown in Table 3. The samples containing acid had lower glass transition temperatures than the sample with no acid, except for the sample with 1.0 wt % HCl. It had a higher glass transition temperature than the sample with no acid.

The narrowing of the transition area to lower temperatures in Figures 8 and 9 indicates that molecular mobility increased, which suggests no dispersion of the linseed oil into the more immobile and rigid inorganic phase during the cross-linking process. In fact, the data in Table 3 indicate that the acid caused less cross-linking to take place and, with the exception of the sample containing 1.0 wt % HCl, caused the glass transition temperature to decrease. One possible explanation for these results could be hydrolysis of the triglycerides in the linseed oil. Under the acidic conditions in the reaction mixture, the triglycerides could have been hydrolyzed to form diglycerides, monoglycerides, glycerol, and fatty acids. This breakdown of the triglycerides would have resulted in less cross-linking and a decrease in the glass transition temperature. Another possible explanation for these results could be

**Figure 10.** Storage modulus ( $E'$ ) as a function of temperature for TEOS/sunflower oil films differing in HCl concentration.

phase separation with the inorganic-rich regions acting as barriers to cross-linking between organic-rich regions dispersed through the sample. Most of the cross-linking would be restricted to the organic-rich regions with few cross-links extending through the inorganic-rich regions into the next organic-rich region. While the cross-link density may be high in the organic-rich regions, the average or effective cross-link density would be lowered by the inorganic regions of low cross-link density. The properties of the sample, such as storage modulus, would be controlled by the average or effective cross-link density. The glass transition temperature would also be lowered by the regions of low cross-link density. The polymer molecules in the organic-rich regions of high cross-link density would not be very mobile, but the polymer molecules extending through the inorganic-rich regions of low cross-link density would be mobile along with entire organic-rich regions, since they are surrounded by regions of low cross-link density.

Figure 10 shows storage modulus ( $E'$ ) as a function of temperature for TEOS/sunflower oil films differing in HCl concentration. The samples containing acid had higher values of high-temperature storage modulus than the sample containing no acid. The sample with 0.5 wt % HCl had the highest value for the high-temperature storage modulus. The minimum values of storage modulus and the corresponding cross-link densities calculated using eq 3 are shown in Table 3. The presence of the acid increased the cross-link density. The sample with 0.5 wt % HCl had the highest cross-link density. The transition regions of the samples containing acid were not as steep as the transition region of the sample



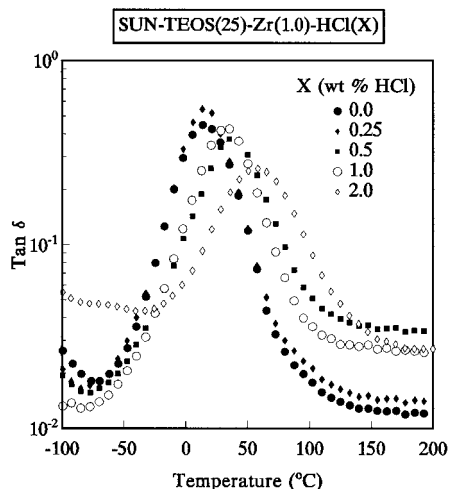


**Figure 11.**  $\tan \delta$  as a function of temperature for TEOS/sunflower oil films differing in HCl concentration.

containing no acid, indicating that the acid broadened the transition region. The transition regions were also shifted to higher temperatures.

$\tan \delta$  is shown in Figure 11 as a function of temperature for TEOS/sunflower oil films differing in HCl concentration. The samples containing acid had broader transition peaks than the sample containing no acid, and the peaks were shifted to higher temperatures. The glass transition temperatures determined from the  $\tan \delta$  peaks are shown in Table 3. The samples containing acid had higher glass transition temperatures than the sample with no acid. The sample with 2.0 wt % HCl had the highest glass transition temperature.

The broadening of the transition area to higher temperatures in Figures 10 and 11 indicates restrictions on molecular mobility, which suggests increased dispersion of the sunflower oil into the more immobile and rigid inorganic phase during the cross-linking process. As more and more of the rigid inorganic phase is incorporated into the organic polymer matrix, the storage modulus, effective cross-link density, and glass transition temperature are increased as shown in Table 3.

SEM and EDAX were used to analyze a LIN-TEOS(25)-Zr(1.0)-HCl(3.0) sample. Figure 12 shows a scanning electron micrograph of raised blisters on the LIN-TEOS(25)-Zr(1.0)-HCl(3.0) sample. The blisters are 100–140  $\mu\text{m}$  in diameter and protrude from the top surface of the coating. Figure 13 shows a higher magnification of a sharply cleaved cross section through a blister of the LIN-TEOS(25)-Zr(1.0)-HCl(3.0) sample. Many fracture planes are visible in the blister region. Figure 14 shows EDAX results for the distribution of atomic silicon through the thickness of a blister region and a nonblister region. The concentration of silicon in the nonblister region was consistent throughout the cross section at 0.2–0.3 atom %. The concentration of silicon in the blister region was very high at the film–substrate interface (1.82 atom %) and decreased out to the top surface of the film (0.23 atom %). This indicates that nucleation of the silicon–oxo clusters may have originated at the film–substrate interface.

Tensile tests indicated that the optimum acid concentration was 1.0 wt % for TEOS/drying oil films. Fracture toughness tests indicated that the optimum

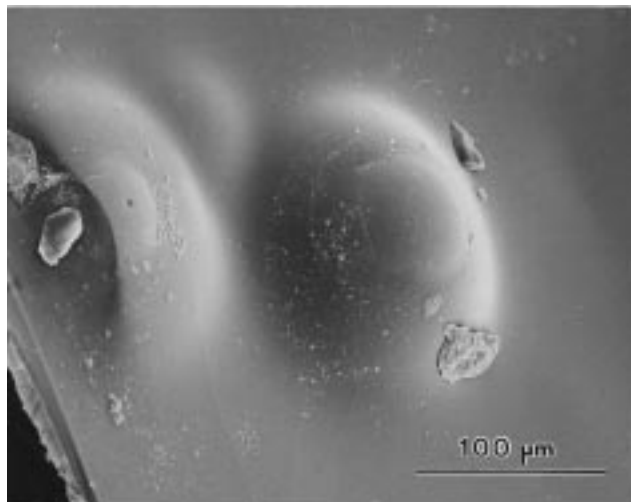


**Figure 12.** Scanning electron micrograph of raised blisters on the surface of the LIN-TEOS(25)-Zr(1.0)-HCl(3.0) sample.

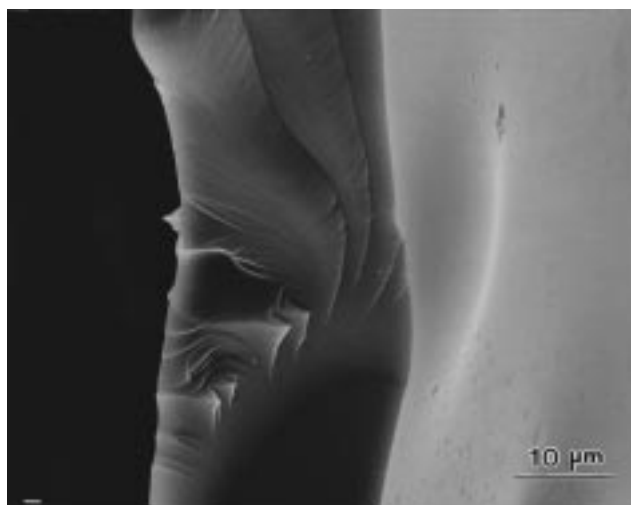


**Figure 13.** Scanning electron micrograph of a sharply cleaved cross section through a blister of the LIN-TEOS(25)-Zr(1.0)-HCl(3.0) sample.

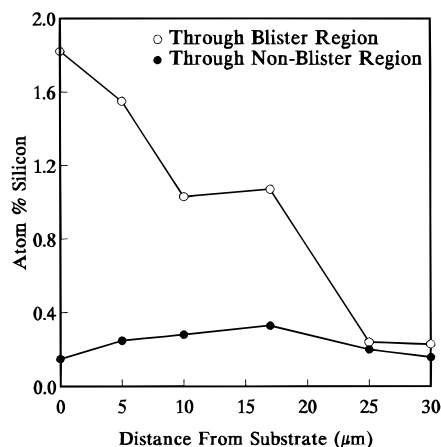


**Figure 14.** EDAX results for atom % silicon in cross sections of blister and nonblister regions of the LIN-TEOS(25)-Zr(1.0)-HCl(3.0) sample. The top surface of the film was located 30  $\mu\text{m}$  from the substrate.

acid concentration for these films was 0.25 wt %. These differing results demonstrate the usefulness of fracture toughness testing. Even though a material can withstand a given tensile load while intact, it may not resist

failure by crack propagation. The TEOS/drying oil films showed a significant increase in the temperature required to produce a 50% weight loss as the acid concentration was increased. Scanning electron microscopy and EDAX results indicate that high acid concentrations can produce phase separation in TEOS/linseed oil films. For a TEOS/linseed oil film with 3.0 wt % HCl, the inorganic-rich regions were 100–140  $\mu\text{m}$  in diameter and contained up to 12 times as much silicon as the rest of the sample.

For TEOS/linseed oil films, DMTA data showed a narrowing of the transition area to lower temperatures as the acid concentration was increased. This indicates that molecular mobility increased and suggests no dispersion of the linseed oil into the more immobile and rigid inorganic phase during the cross-linking process. Increasing the acid concentration caused the cross-link density and the glass transition temperature to decrease. These results can be explained by hydrolysis of the triglycerides in the linseed oil or phase separation with the inorganic-rich regions acting as cross-link barriers.

For TEOS/sunflower oil films, DMTA data showed a broadening of the transition area to higher temperatures as the acid concentration was increased. This indicates that molecular mobility decreased and suggests increased dispersion of the sunflower oil into the more immobile and rigid inorganic phase during the cross-linking process. Increasing the acid concentration caused the cross-link density and the glass transition temperature to increase as more and more of the rigid inorganic phase was incorporated into the organic polymer matrix.

## Conclusions

The acid catalyst had an effect on the morphology and thermomechanical properties of the drying-oil-based inorganic–organic hybrid materials. Higher acid concentrations led to larger inorganic phases. Using 3.0 wt % HCl in a TEOS/linseed oil film produced inorganic regions with diameters as large as 140  $\mu\text{m}$  and silicon concentrations up to 12 times higher than the rest of the sample. For the same catalytic conditions, the linseed oil-based hybrid materials exhibited better mechanical properties than the sunflower oil-based hybrid materials. Tensile strength and modulus generally increased with increasing acid concentration. The maximum tensile properties were obtained with 1.0 wt % HCl. The maximum fracture toughness was obtained from a linseed oil-based hybrid material containing 0.25 wt % HCl. The best balance of properties was also obtained from the linseed oil-based hybrid material catalyzed with 0.25 wt % HCl.

**Acknowledgment.** The authors wish to thank the United States Department of Agriculture (USDA) for the financial support required for this research (Grant #94-34216-0031). They also wish to thank C.P. Chang of the Composite Research Laboratories at Auburn University for the fracture toughness measurements, and the members of the USDA Northern Crop Science Laboratory at North Dakota State University for the SEM and EDAX measurements. Special thanks are also extended to Frost Paint and Oil Corp. (Chicago, IL) and National Sun Industries (Fargo, ND) for providing the seed oils.

CM980606A